Link Between Autumnal Arctic Sea Ice and Northern Hemisphere Winter Forecast Skill

J. C. Acosta Navarro, P. Ortega, L. Batté, D. Smith, P. A. Bretonnière, V. Guemas, F. Massonnet, V. Sicardi, V. Torralba, E. Tourigny, et al.

AGU100 ADVANCING EARTH AND SPACE SCIENCE

Geophysical Research Letters

RESEARCH LETTER
10.1029/2019GL086753

Link Between Autumnal Arctic Sea Ice and Northern Hemisphere Winter Forecast Skill

J. C. Acosta Navarro[1], P. Ortega[1], L. Batté[2], D. Smith[3], P. A. Bretonnière[1], V. Guemas[2], F. Massonnet[1,4], V. Sicardi[1], V. Torralba[1], E. Tourigny[1], and F. J. Doblas-Reyes[1,5]

[1]Barcelona Supercomputing Center, Barcelona, Spain, [2]CNRM UMR 3589, Université de Toulouse, Météo-France, CNRS, Toulouse, France, [3]Met Office Hadley Centre, Exeter, UK, [4]Georges Lemaître Centre for Earth and Climate Research, Earth and Life Institute, Université catholique de Louvain, Louvain-la-Neuve, Belgium, [5]Catalan Institution for Research and Advanced Studies (ICREA), Barcelona, Spain

Key Points:
- Climate forecast systems have limited predictive capacity at seasonal scales in the Northern Hemisphere midlatitudes
- Autumnal Barents and Kara Sea ice is likely a source of winter climate predictability in large regions of northern Eurasia
- Analysis of multimodel initialized predictions suggests that winter predictability in Eurasia is enhanced by a sea ice-atmosphere linkage

Supporting Information:
- Supporting Information S1

Correspondence to:
J. C. Acosta Navarro,
jacosta@bsc.es

Citation:
Acosta Navarro, J. C., Ortega, P., Batté, L., Smith, D., Bretonnière, P. A., Guemas, V., et al. (2020). Link between autumnal Arctic sea ice and Northern Hemisphere winter forecast skill. *Geophysical Research Letters*, *47*, e2019GL086753. https://doi.org/10.1029/2019GL086753

Received 25 DEC 2019
Accepted 12 FEB 2020
Accepted article online 14 FEB 2020

The copyright line for this article was changed on 1 DEC 2020 after original online publication.

Abstract Dynamical forecast systems have low to moderate skill in continental winter predictions in the extratropics. Here we assess the multimodel predictive skill over Northern Hemisphere high latitudes and midlatitudes using four state-of-the-art forecast systems. Our main goal was to quantify the impact of the Arctic sea ice state during November on the sea level pressure (SLP), surface temperature, and precipitation skill during the following winter. Interannual variability of the November Barents and Kara Sea ice is associated with an important fraction of December to February (DJF) prediction skill in regions of Eurasia. We further show that skill related to sea ice in these regions is accompanied with enhanced skill of DJF SLP in western Russia, established by a sea ice-atmosphere teleconnection mechanism. The teleconnection is strongest when atmospheric blocking conditions in Scandinavia/western Russia in November reduce a systematic SLP bias that is present in all systems.

Plain Language Summary There is a broad range of stakeholders that could benefit from Northern Hemisphere, midlatitude winter climate predictions from dynamical forecast systems. However, a widespread use is currently hindered by important forecast system limitations. The results from this study suggest that autumnal Arctic sea ice state may have an important impact on winter climate forecast capacity in parts of Eurasia. We further show that large ensembles of simulations can be further exploited, by identifying the members with a better representation of certain processes, in this case the teleconnection between Arctic sea ice and the atmospheric circulation, to enhance the prediction skill of temperature and precipitation over the continents. Exploring this approach for other regions and seasons can provide a possible pathway toward more human-relevant seasonal climate predictions.

Introduction

The Arctic region is undergoing a profound transformation: in the past four decades, the Arctic has warmed twice as fast as the global average (Overland et al., 2015), due to the effect of Arctic amplification (Pithan & Mauritsen, 2014). In addition, the annual minimum sea ice extent (September) has halved, and Arctic marginal Seas at present experience longer ice-free conditions than before (Perovich et al., 2019). The quickly evolving climatic conditions have already led to ecological and social changes in the region (Meier et al., 2014; Post et al., 2013). Unless strong globally coordinated greenhouse gas mitigation policies are implemented in the coming years, climate projections suggest that the Arctic will continue to warm by several degrees by midcentury, possibly leading, at that time, to seasonally ice-free Arctic conditions during the late summer/early autumn (Collins et al., 2013).

Scientific and nonscientific interest in the remote effects of Arctic warming and sea ice loss on midlatitude weather and climate has quickly grown in the last decade. The World Climate Research Program included the "melting ice and its global consequences" as one if its Grand Challenges (www.wcrp-climate.org/gc-melting-ice-global-consequences). While there is observationally based evidence that Arctic warming and in particular sea ice loss have led to changes in the climate conditions at the midlatitudes (Mori et al., 2019), the findings are not conclusive (Blackport et al., 2019), and the large natural variability together with the relatively short time covered by observational records may still forbid distinguishing the signal from the noise (Jung et al., 2015).

Despite the limitations found in analyses based on observational data, sensitivity experiments with climate models of different complexity indicate that sea ice loss can indeed drive large-scale changes in northern midlatitude circulation on time scales that span from days to centuries (Cohen et al., 2014; Mori et al., 2019; Screen et al., 2018; Semmler et al., 2018). Sea ice loss induces a local warming that is strongest in autumn and winter, the seasons during which sea ice is thought to exert the largest influence on midlatitudinal climate. As sea ice retreats, the warmer ocean is no longer insulated from the colder atmosphere, which induces local anomalous atmospheric diabatic heating near the surface and in turn excites Rossby waves that may cause climatic effects at midlatitudes (Honda et al., 2009; Mori et al., 2014). Studies have shown that a low Arctic sea ice cover may be partly responsible for winter drought conditions in California (Cvijanovic et al., 2017) and extreme cold episodes in East Asia (Honda et al., 2009) and eastern North America (Kug et al., 2015). In particular, García-Serrano et al. (2015) and Acosta Navarro et al. (2019) found that autumnal sea ice conditions in the Barents and Kara Seas could induce changes in the Euro-Atlantic climate in the following season, which suggests that sea ice state in autumn is a predictor for winter climate (Kretschmer et al., 2016).

An important fraction of skill in seasonal climate predictions using forecast systems stems from model initialization (Meehl et al., 2009). Forecast system initialization synchronizes the model climate with the observed one by phasing their respective natural climate signal and by reducing the differences in their initial states. This yields subseasonal to decadal predictability through initialization of slowly evolving components of the climate system (i.e., components with persistence such as the ocean, sea ice, or land). As an example, incorporating Arctic observations in the initialization of predictions leads to better subseasonal (Jung et al., 2014; Semmler et al., 2018) and seasonal (Elders & Pegion, 2019) forecasts at midlatitudes. Overland et al. (2016) suggest that enhanced predictive capability in the Arctic and beyond can be achieved through improved model initialization together with the use of multiple forecast systems in a coordinated framework, further expanding the current understanding of the effects of a changing Arctic on midlatitudes.

The main aim of this study is to explore in a multimodel framework the added value attributable to Arctic sea ice conditions during November (month of initialization) on December to February (DJF) sea level pressure (SLP), surface (2-m) air temperature (SAT), and precipitation skill. Our experiments cover a recent period of strong Arctic warming (1993-2014), increased sea ice extent variability (Goosse et al., 2009), and comprehensive observational coverage to evaluate forecast skill.

Materials and Methods

Models and Observations

Our analysis includes four contemporary seasonal forecast systems built from the fully coupled atmosphere-land-ocean-sea ice models: BSC's EC-Earth3.2 (Doblas-Reyes et al., 2018; Manubens-Gil et al., 2016), CNRM and CERFACS CNRM-CM6-1 (Voldoire et al., 2019), Met Office's GloSea5-v13 (MacLachlan et al., 2015), and ECMWF's SEAS5 (Johnson et al., 2019). To give equal weight to each system in terms of total number of forecast members, 6-month reforecasts with 25 members per system were initialized every 1 November (or close to 1 November in the case of GloSea5, supporting information Table S1) over the period 1993–2014. The analysis is focused on the DJF averages. The atmospheric components in all four forecast systems were initialized from ERA-Interim states (Dee et al., 2011) interpolated to the model's own grid. The ocean and sea ice components in CNRM-CM6-1 were initialized from an ocean-sea ice simulation with temperature, salinity, and sea ice concentration nudged toward GLORYS-2V4 reanalysis (Ferry et al., 2010) and relaxation time of ~2 days; in GloSEA5 ocean and sea ice were initialized directly from NEVOMAR reanalysis (Mogensen et al., 2012) states; and in SEAS5 they were initialized directly from ORAS5 reanalysis (Zuo et al., 2019) states. The ocean and sea ice models used to generate initial conditions for CNRM-CM6-1, GloSEA5, and SEAS5 are the same as in the respective coupled versions used to produce the forecasts. The ocean component of EC-Earth3.2 was initialized from interpolated ORAS4 (Balmaseda et al., 2013) states and the sea ice component from an ocean-sea ice simulation in which sea ice concentration from EUMETSAT/OSI-SAF is assimilated at the beginning of each month using an ensemble Kalman filter (Massonnet et al., 2014, Table S1). Small perturbations around the initial state of the ocean, atmosphere, and sea ice were used to initialize the respective components of each forecast system and generate different ensemble members.

For verification purposes, observed GPCP v2.2 precipitation (Adler et al., 2003; Huffman et al., 2009), surface (2-m) temperature and SLP from the ERA-Interim reanalysis (Dee et al., 2011), and observed sea ice concentrations from Centre de Recherche et d'Exploitation Satellitaire (CERSAT) were considered (http://cersat.ifremer.fr/data/products/catalogue) as references. Before the analysis, both seasonal forecasts and observational references have been regridded from their original grid to a common regular grid of about 2.5° × 2.5° to match the coarsest GPCP v2.2 grid. The scripts used to generate the plots in this article are available upon request and are largely based on the s2dverification R package (Manubens et al., 2018).

Choice of the Study Region

The Barents and Kara Seas have large climate variability during autumn and may play a role in winter climate in Eurasia by affecting the Siberian anticyclone and/or the North Atlantic oscillation (NAO; Honda et al., 2009; Kug et al., 2015; García-Serrano et al., 2015; Zhang et al., 2018). For that reason, a correct initialization of the Barents and Kara Sea ice (BKSI) in November can potentially benefit the skill of the winter atmospheric circulation and surface climate conditions. The Barents and Kara Seas region (here defined as the area between 15–100°E and 65–80°N, black boxes in Figure 2) is used in this work to investigate if the BKSI variability, and predictive capacity affects the climate predictability at the midlatitudes. A similar analysis but for the whole Arctic and other individual regions, like the Chukchi and East Siberian Seas, has also been performed, but their contribution to midlatitude climate predictability was nonsignificant.

Methodological Approach

Most studies have investigated the Arctic midlatitude teleconnection using idealized experiments or different forms of statistical analysis on observations to explain the underlying mechanisms (Jung et al., 2015). Here we follow a novel approach to evaluate how the sea ice state during November influences DJF climate predictability using four state-of-the-art seasonal prediction systems (i.e., initialized climate models). In each seasonal prediction system, the skill of the main large-scale variables (i.e., SLP, SAT, and precipitation) is computed twice, before and after regressing out the November sea ice induced variability (described in the following section). By comparing these two skill estimates and assuming linearity, we can thus quantify which part of the skill is related to the November sea ice. Before computing skill, the forecasts are bias corrected by removing the mean ensemble climatology for each member. Skill is quantified here as the temporal anomaly correlation between the forecast ensemble mean and the observation for each variable. Multimodel mean values are computed as the mean of the hundred ensemble members from the four forecasts systems (25 members each).

Quantifying the Role of Barents-Kara Sea Ice

To understand the marginal role of BKSI on DJF climate predictions, the following procedure is applied: The driving signal from the BKSI index is estimated as the linearly detrended November sea ice area anomaly in the Barents-Kara Seas. Similar final findings (not shown) are also derived in this work from an equivalent index based on the sea ice extent or by detrending the series using a second-degree polynomial. This signal is computed in both the observations and the seasonal forecasts. The detrending allows us to focus on the year-to-year variability over the region and prevent any overinterpretation based on common long-term trends, which might not be physically linked. The ensemble mean, linearly detrended index is then regressed on the ensemble mean DJF SLP, SAT, and precipitation anomalies in each system, to characterize the response of these climate variables to sea ice variability.

The ensemble mean November BKSI-related linear signal is then removed from the nondetrended DJF SLP, SAT, and precipitation anomaly field for every system by subtracting the product of the BKSI index and the regressed fields along the temporal dimension. The resulting fields (after BKSI signal removal) are used in the following as another set of seasonal predictions without the interannual variability that can be linked to the November BKSI. Similar results are found (not shown), if the BKSI signal removal procedure is done using individual ensemble members, instead of ensemble mean.

In all scatterplots (Figure 3), each point is estimated using a bootstrap method calculating the ensemble mean of a randomly sampled 10-member subensemble from each forecast system. The process is repeated 1,000 times, which provides 1,000 correlation values for each system.

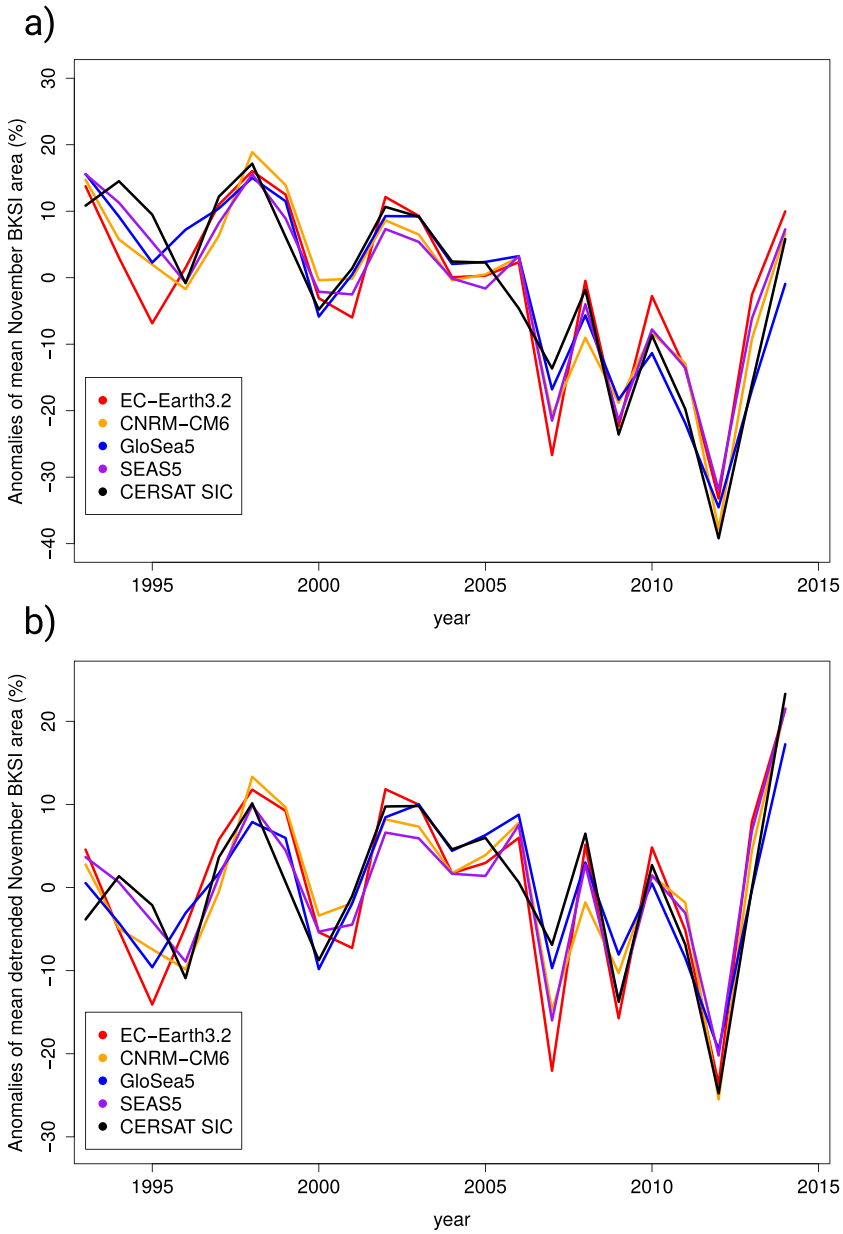

Figure 1. Sea ice cover anomalies over the Barents and Kara Seas (BKSI) in November. (a) Ensemble mean forecasts initialized every 1 November in each individual system (colors) and in the observational reference (black). (b) Same as (a) but after linearly detrending the November BKSI index.

Results

The four forecast systems accurately represent the decline and year-to-year variability of sea ice cover in the Barents and Kara Seas in the first month after forecast initialization (Figures 1a and 1b). The anomaly correlation coefficient with CERSAT reference data is indeed high for all forecast systems in November: over 0.85 and 0.8, before and after linearly detrending, respectively. Likewise, the mean DJF anomaly correlation coefficient is also high with respective values of 0.8 and 0.6 for the nondetrended and detrended data from the different seasonal forecast systems, respectively.

Comparing the multimodel forecasts with and without the signal related to the November BKSI index shows that the Barents-Kara region is associated with enhanced and degraded skill in DJF SLP skill (temporal correlation) in the northern and southern North Atlantic regions, respectively (Figures 2a and 2b). There is a

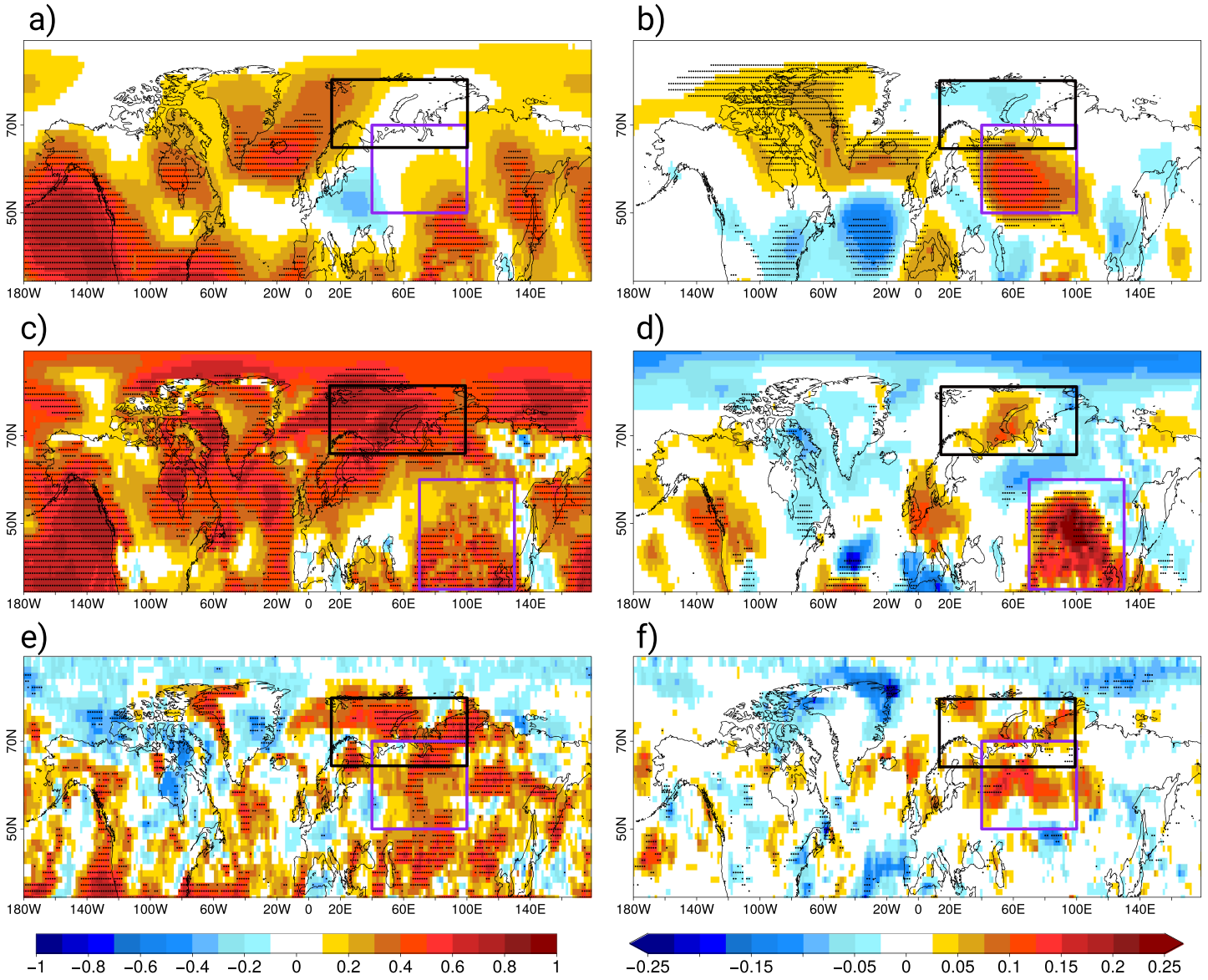

Figure 2. Skill (linear correlation) in multimodel mean DJF (a) sea level pressure, (c) surface air temperature, and (e) precipitation anomalies. Skill impact (difference in correlation between the set of forecasts with and without the November BKSI index signal) of the November BKSI cover in multimodel means of DJF (b) sea level pressure, (d) surface air temperature, and (f) precipitation anomalies. Dots indicate statistically significant values at the 0.05 confidence using a two-sided *T* test. Purple boxes in (a), (b), (e), and (f) represent western Russia, and northern central and East Asia in (c) and (d), which are the regions with the maximum gain in skill. The black box shows the Barents-Kara region.

significant positive difference in skill of more than 0.1 in western Russia, but it is important to notice that in this region the multimodel mean exhibits only marginal skill (Figure 2a). However, looking at single models shows that the two models with the highest skill in western Russia, EC-Earth3.2 and, especially, GloSea5, also show the strongest increase in skill in that region reaching values of over 0.2 (Figures S1 and S2). Those results are consistent with other forecast quality metrics such as the root-mean-square error (Figures S3 and S4). The other two models, SEAS5 and especially CNRM-CM6-1, show a positive impact on skill but displaced to the North Atlantic sector.

In terms of SAT, all models show a coherent pattern with positive BKSI-related skill in northern central and East Asia (Figures 2c, 2d, S5, and S6), likely associated with the respective skill gain in atmospheric circulation over western Russia. There is a smaller effect of sea ice on SAT skill over Europe and North America. Skill in precipitation is positively affected over western Russia in all models, the region where the impact

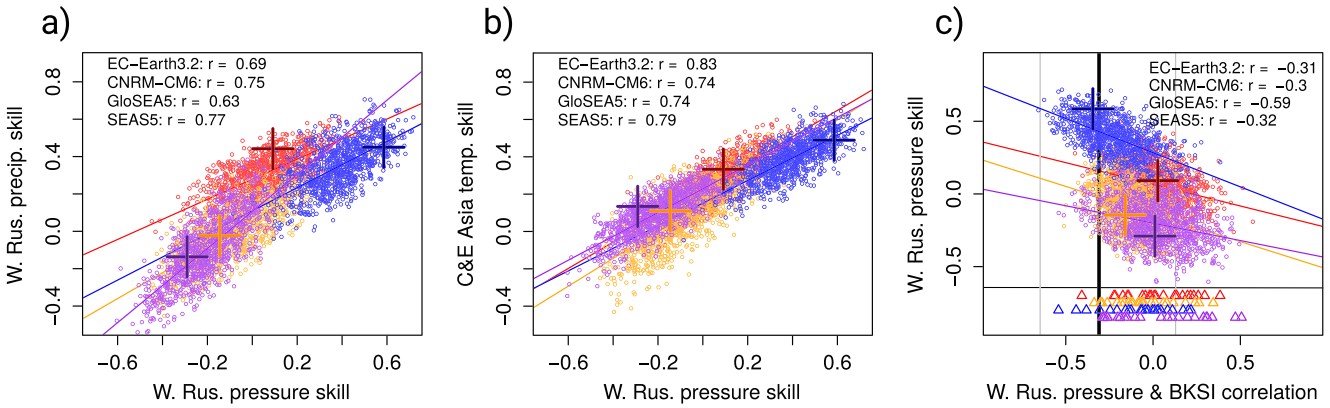

Figure 3. Scatterplots with the DJF skill relationship between (a) sea level pressure (*x* axis) and precipitation (*y* axis) in western Russia, (b) sea level pressure in western Russia (*x* axis) and surface air temperature in northern central and East Asia (*y* axis), and (c) the correlation between western Russia sea level pressure and November BKSI index (*x* axis) and the skill in western Russia SLP (*y* axis). Red, yellow, blue, and purple points display values from EC-Earth3.2, CNRM-CM6-1, GloSea5, and SEAS5, respectively. All displayed *r* values are significantly different from 0 at the 0.05 confidence level using a one-sided *T* test after a Fisher transformation. The dark colored crosses represent the values from the full ensembles, while the triangles at the bottom represent the strength of the teleconnection of individual ensemble members. The black and gray vertical lines show the mean and 95% confidence interval of the correlation between ERA-Interim sea level pressure and CERSAT sea ice cover, respectively.

on SLP is also the strongest (Figures 2e, 2f, S7, and S8). Despite the moderate DJF SLP, SAT, and precipitation forecast skill over midlatitude land regions found in dynamical forecast systems (Figures 2a, 2c, and 2e), persistence forecasts using November observed/reanalyzed anomalies (Figure S9) have a considerably lower skill, including the regions of BKSI influence.

To establish whether and how DJF SLP in western Russia (purple box in Figure 2a), precipitation in the same region, temperature in central/East Asia (purple box in Figure 2c), and November BKSI (black box in Figure 2b) are interrelated, we perform a bootstrap analysis, subselecting 10 members from each of the original forecast systems (i.e., without the BKSI signal removed), and repeat the process 1,000 times to investigate the relationships between the different skill estimates. The scatterplots in Figures 3a and 3b show that, indeed, subensembles with higher skill in SLP in western Russia consistently show higher skill in precipitation over the region, and surface temperature in central/East Asia. These linear relationships are significant at the 0.05 confidence level for all forecast systems, thus supporting atmospheric circulation as a fundamental player in determining winter climate variability in those regions.

The direct link between a higher skill in November BKSI and a higher skill in western Russia DJF SLP is however not significant (not shown). This does not exclude BKSI as a key contributor to atmospheric circulation variability and skill in western Russia, but it suggests that its influence may be nonlinear. Indeed, a large body of literature supports that reduced Barents-Kara sea ice cover during autumn induces positive anomalies in winter SLP over western Russia (Honda et al., 2009; Mori et al., 2014; Zhang et al., 2018).

Figure 3c shows a different scatterplot, this time linking the strength of the teleconnection between November BKSI and western Russia winter SLP with the skill in the latter. It also indicates, in a vertical bar, the strength of this teleconnection (characterized as the correlation coefficient between both indices) as diagnosed from observations. Interestingly, in all systems, subensembles with a stronger teleconnection tend to have higher skill in the western Russia atmospheric circulation. This linear relationship is significant for all systems, but it does not imply causality as the influence of external common drivers cannot be excluded. Similarly, for each forecast system, a higher skill in DJF surface temperature in northern central and East Asia and in DJF precipitation in western Russia are found in random subsamples of members that have a stronger teleconnection between November BKSI and western Russia DJF SLP (Figure S10). It is important to notice that the teleconnection in all systems lies within the observed uncertainty range, with GloSea5 being closest to observations. Additionally, GloSea5 is the model with the highest baseline skill in SLP in western Russia.

To understand why a stronger teleconnection leads to higher skill in the large-scale atmospheric circulation, and by extension in precipitation over Russia and temperature further southeast, we compare the typical

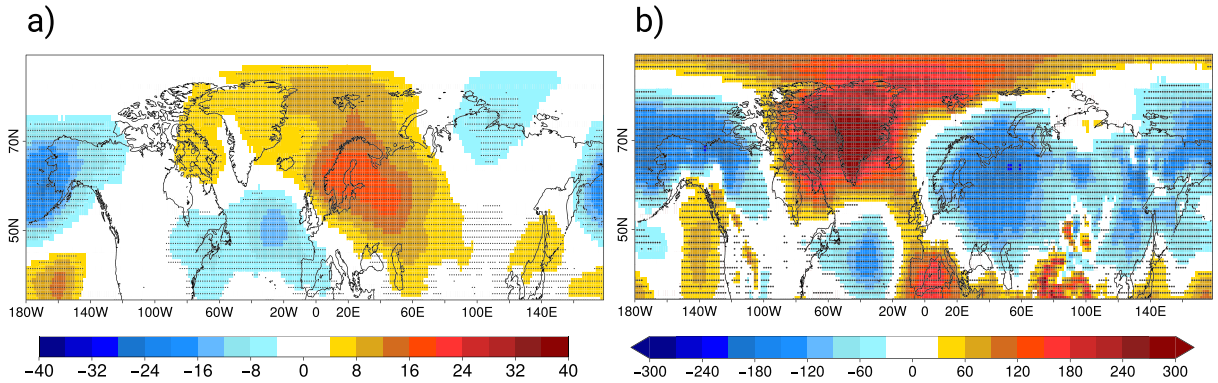

Figure 4. (a) Difference in multimodel November sea level pressure (Pa) of the top and bottom 10% random subensembles with strongest and weakest anticorrelation between DJF sea level pressure in west Russia and November BKSI index, respectively. (b) Multimodel mean November sea level pressure bias (Pa). Dots indicate statistically significant values at the 0.05 confidence level using a two-sided *T* test.

surface circulation conditions in the members with the strongest and weakest teleconnection. Composites of anomalies in November SLP computed as the mean difference of the 10-member subensembles in each system with 10% strongest and 10% weakest anticorrelation between DJF SLP in western Russia and November BKSI index (see Figure 3c), reveal a clear Scandinavian blocking pattern in November, with additional anomalous cyclonic circulation over the North Atlantic and North Pacific regions (Figure 4a). A similar blocking situation has been found to foster the linkage between the Arctic and northern Asian winter weather conditions on weekly time scales (Day et al., 2019). Similar processes might be behind the increased western Russia SLP skill observed in our systems when the teleconnection is strongest. It should be noted that SLP in the Scandinavian/western Russian region presents important negative biases in all models (Figures 4b and S11), and all forecast systems show a stronger teleconnection in the random ensemble member subsets that reduce the bias (Figure 3c).

Discussion and Conclusions

Previous studies have found that the sea ice variability in the Barents-Kara region during autumn exerts an influence on mean winter SLP and SAT in large areas of northern Eurasia. Our results support this by showing that filtering out the signal explained by detrended BKSI anomalies in November significantly degrades skill in predictions of winter (DJF) SLP and precipitation in western Russia and SAT in northern central and East Asia. The results obtained show that multimodel skill for SLP, SAT, and precipitation in the regions of BKSI influence is substantially larger than for persistence forecasts, revealing an added value of dynamical forecast systems over the most basic statistical forecasts.

A bootstrap analysis subsampling different forecast members allowed us to establish a link between the skill in western Russia SLP and the skill in the local precipitation and central/Eastern Asia temperature. The impact of BKSI on the north and central Asian climate skill involves a teleconnection mechanism whose strength depends on atmospheric blocking conditions over Scandinavia/west Russia during November. Such blocking conditions also help to reduce the magnitude of the November negative SLP bias in the region that is present in all forecast systems.

To sum up, our results indicate that sea ice cover in the Barents and Kara Seas during autumn is a source of winter climate predictability at midlatitudes in Eurasia. Our results further suggest that improving sea ice representation, its teleconnections, and systematic bias reduction in climate models could possibly result in additional seasonal prediction skill over the surrounding continents, a task that has proven to be challenging. Previous studies have shown important progress in predicting Euroatlantic winter climate related to skillful NAO seasonal predictions (Dobrynin et al., 2018; Scaife et al., 2014). Our findings suggest that BKSI may be a complementary source of winter climate predictability in regions of low impact of other dominant climatic modes of variability in the Northern Hemisphere midlatitudes.

In this study we used large ensembles of initialized simulations (25 per system) in a multimodel framework, which allowed us to detect a robust signal on surface climate by averaging out atmospheric noise. Despite the

observed improvement in the seasonal predictions by including the BSKI-related signal, the results should be interpreted with caution since the skill gain is in some cases a small fraction of the baseline skill. In addition, the role of the ocean and/or land as possible common drivers of sea ice variability in November and continental winter climate has not been directly addressed in this study, and the period of reforecast evaluation covers only 22 years. Furthermore, whereas the impact of Arctic sea ice changes on the atmosphere is likely nonlinear, the method used in this study to remove the BKSI signal of the forecasts is a linear approximation, which could lead to an underestimation of the role of BKSI. Applying a nonlinear method was, however, discarded to avoid any risk of overfitting (due to the short data training period).

For these reasons, we will explore in the future a set of coordinated multimodel sensitivity experiments in prediction mode focusing on the BKSI and covering a longer period of time. Additionally, analysis of the Polar Amplification Model Intercomparison Project (Smith et al., 2019) experiments targeting sea ice loss in the Barents and Kara Seas and other regions will possibly shed light on the elusive causal linkages connecting polar and midlatitude regions.

Acknowledgments
This work was funded by the European Union projects APPLICATE (Grant 727862), PRIMAVERA (Grant 641727), INTAROS (Grant 727890), and ESA/CMUG-CCI3. We acknowledge PRACE for awarding us access to MareNostrum IV at Barcelona Supercomputing Center (BSC), Spain. J. C. A. N. received financial support from the Spanish Ministerio de Ciencia, Innovación y Universidades through a Juan de la Cierva personal grant (FJCI-2017-34027). E. T. received funding from the European Union's Horizon 2020 research and innovation program under the Marie Skłodowska-Curie grant Agreement 748750 (SPFireSD project). V. G. received funding from the Agence Nationale de la Recherche through the Make Our Planet Great Again Grant ANR-17-MPGA-003. The data from EC-Earth3.2 and CNRM-CM6-1 are publicly available (at https://applicate.eu/data/data-portal). GloSea5 (v13) and SEAS5 data are publicly available (at https://cds.climate.copernicus.eu/cdsapp#!/dataset/seasonal-monthly-single-levels?tab=overview). All the data were downloaded from their original source, converted to NetCDF in a format designed for efficient analysis with the tools mentioned before, and quality checked at several levels.

References

Acosta Navarro, J. C., Ortega, P., García-Serrano, J., Guemas, V., Tourigny, E., Cruz-García, R., et al. (2019). December 2016: Linking the lowest Arctic sea-ice extent on record with the lowest European precipitation event on record. *Bulletin of the American Meteorological Society*, *100*, S43–S48. https://doi.org/10.1175/BAMS-D-18-0097.1

Adler, R. F., Huffman, G. J., Chang, A., Ferraro, R., Xie, P. P., Janowiak, J., et al. (2003). The version-2 global precipitation climatology project (GPCP) monthly precipitation analysis (1979–present). *Journal of Hydrometeorology*, *4*(6), 1147–1167. https://doi.org/10.1175/1525-7541(2003)004<1147:TVGPCP>2.0.CO;2

Balmaseda, M. A., Mogensen, K., & Weaver, A. T. (2013). Evaluation of the ECMWF ocean reanalysis system ORAS4. *Quarterly Journal of the Royal Meteorological Society*, *139*, 1132–1161. https://doi.org/10.1002/qj.2063

Blackport, R., Screen, J. A., van der Wiel, K., & Bintanja, R. (2019). Minimal influence of reduced Arctic sea ice on coincident cold winters in mid-latitudes. *Nature Climate Change*, *9*, 697–704. https://doi.org/10.1038/s41558-019-0551-4

CERSAT: These data were obtained from the Centre de Recherche et d'Exploitation Satellitaire (CERSAT) (n.d.) at IFREMER, Plouzané (France): ftp://ftp.ifremer.fr/ifremer/cersat/products/gridded/psi-concentration/data/arctic

Cohen, J., Screen, J. A., Furtado, J. C., Barlow, M., Whittleston, D., Coumou, D., et al. (2014). Recent Arctic amplification and extreme mid-latitude weather. *Nature Geoscience*, *7*, 627–637. https://doi.org/10.1038/ngeo2234

Collins, M., Knutti, R., Arblaster, J., Dufresne, J.-L., Fichefet, T., Friedlingstein, P., et al. (2013). *Long-term climate change: Projections, commitments and irreversibility. Climate Change 2013—The physical science basis: Contribution of Working Group I to the Fifth Assessment Report of the Intergovernmental Panel on Climate Change* (Vol. *2013*, pp. 1029–1136). Cambridge: Cambridge University Press.

Cvijanovic, I., Santer, B. D., Bonfils, C., Lucas, D. D., Chiang, J. C. H., & Zimmerman, S. (2017). Future loss of Arctic sea-ice cover could drive a substantial decrease in California's rainfall. *Nature Communications*, *8*, 1947. https://doi.org/10.1038/s41467-017-01907-4

Day, J. J., Sandu, I., Magnusson, L., Rodwell, M. J., Lawrence, H., Bormann, N., & Jung, T. (2019). Increased Arctic influence on the midlatitude flow during Scandinavian Blocking episodes. *Quarterly Journal of the Royal Meteorological Society*, *145*, 3846–3862. https://doi.org/10.1002/qj.3673

Dee, D. P., Uppala, S. M., Simmons, A. J., Berrisford, P., Poli, P., Kobayashi, S., et al. (2011). The ERA-Interim reanalysis: Configuration and performance of the data assimilation system. *Quarterly Journal of the Royal Meteorological Society*, *137*, 10980. https://doi.org/10.1002/qj.828

Doblas-Reyes, F. J., Navarro, J. C. A., Batté, L., Volpi, D., Acosta, M., Bellprat, O., et al. (2018). Using EC-Earth for climate prediction research. *ECMWF Newsletter (ECMWF)*, *154*, 35–40. https://doi.org/10.21957/fd9kz3

Dobrynin, M., Domeisen, D. I. V., Müller, W. A., Bell, L., Brune, S., Bunzel, F., et al. (2018). Improved teleconnection-based dynamical seasonal predictions of boreal winter. *Geophysical Research Letters*, *45*, 3605–3614. https://doi.org/10.1002/2018GL077209

Elders, A., & Pegion, K. (2019). Diagnosing sea ice from the north american multi model ensemble and implications on mid-latitude winter climate. *Climate Dynamics*, *53*(12), 7237–7250. https://doi.org/10.1007/s00382-017-4049-3

Ferry, N., Parent, L., Garric, G., Barnier, B., & Jourdain, N. C. (2010). Mercator global Eddy permitting ocean reanalysis GLORYS1V1: Description and results. *Mercator-Ocean Quarterly Newsletter*, *36*, 15–27.

García-Serrano, J., Frankignoul, C., Gastineau, G., & de la Cámara, A. (2015). On the predictability of the winter Euro-Atlantic climate: Lagged influence of autumn Arctic sea ice. *Journal of Climate*, *28*, 5195–5216. https://doi.org/10.1175/JCLI-D-14-00472.1

Goosse, H., Arzel, O., Bitz, C. M., de Montety, A., & Vancoppenolle, M. (2009). Increased variability of the Arctic summer ice extent in a warmer climate. *Geophysical Research Letters*, *36*, L23702. https://doi.org/10.1029/2009GL040546

Honda, M., Inoue, J., & Yamane, S. (2009). Influence of low Arctic sea-ice minima on anomalously cold Eurasian winters. *Geophysical Research Letters*, *36*, L08707. https://doi.org/10.1029/2008GL037079

Huffman, G. J., Adler, R. F., Bolvin, D. T., & Gu, G. (2009). Improving the global precipitation record: GPCP version 2.1. *Geophysical Research Letters*, *36*, L17808. https://doi.org/10.1029/2009GL040000

Johnson, S. J., Stockdale, T. N., Ferranti, L., Balmaseda, M. A., Molteni, F., Magnusson, L., et al. (2019). SEAS5: The new ECMWF seasonal forecast system. *Geoscientific Model Development*, *12*, 1087–1117. https://doi.org/10.5194/gmd-12-1087-2019

Jung, T., Doblas-Reyes, F., Goessling, H., Guemas, V., Bitz, C., Buontempo, C., et al. (2015). Polar lower-latitude linkages and their role in weather and climate prediction. *Bulletin of the American Meteorological Society*, *96*, ES197–ES200. https://doi.org/10.1175/BAMS-D-15-00121.1

Jung, T., Kasper, M. A., Semmler, T., & Serrar, S. (2014). Arctic influence on subseasonal midlatitude prediction. *Geophysical Research Letters*, *41*, 3676–3680. https://doi.org/10.1002/2014GL059961

Kretschmer, M., Coumou, D., Donges, J. F., & Runge, J. (2016). Using causal effect networks to analyze different Arctic drivers of midlatitude winter circulation. *Journal of Climate*, *29*, 4069–4081. https://doi.org/10.1175/JCLI-D-15-0654.1

Kug, J.-S., Jeong, J. H., Jang, Y. S., Kim, B. M., Folland, C. K., Min, S. K., & Son, S. W. (2015). Two distinct influences of Arctic warming on cold winters over North America and East Asia. *Nature Geoscience*, *8*, 759–762. https://doi.org/10.1038/ngeo2517

MacLachlan, C., Arribas, A., Peterson, K. A., Maidens, A., Fereday, D., Scaife, A. A., et al. (2015). Global Seasonal forecast system version 5 (GloSea5): A high-resolution seasonal forecast system. *Quarterly Journal of the Royal Meteorological Society*, *141*, 1072–1084. https://doi.org/10.1002/qj.2396

Manubens, N., Caron, L. P., Hunter, A., Bellprat, O., Exarchou, E., Fučkar, N. S., et al. (2018). An R package for climate forecast verification. *Environmental Modelling & Software*, *103*, 29–42. https://doi.org/10.1016/j.envsoft.2018.01.018

Manubens-Gil, D., Vegas-Regidor, J., Prodhomme, C., Mula-Valls, O., & Doblas-Reyes, F. J. (2016). Seamless management of ensemble climate prediction experiments on HPC platforms. 2016 International Conference on High Performance Computing & Simulation (HPCS). IEEE.

Massonnet, F., Goosse, H., Fichefet, T., & Counillon, F. (2014). Calibration of sea ice dynamic parameters in an ocean-sea ice model using an ensemble Kalman filter. *Journal of Geophysical Research: Oceans*, *119*, 4168–4184. https://doi.org/10.1002/2013JC009705

Meehl, G. A., Goddard, L., Murphy, J., Stouffer, R. J., Boer, G., Danabasoglu, G., et al. (2009). Decadal prediction: Can it be skillful? *Bulletin of the American Meteorological Society*, *90*(10), 1467–1486. https://doi.org/10.1175/2009BAMS2778.1

Meier, W. N., Hovelsrud, G. K., van Oort, B. E. H., Key, J. R., Kovacs, K. M., Michel, C., et al. (2014). Arctic sea ice in transformation: A review of recent observed changes and impacts on biology and human activity. *Reviews of Geophysics*, *52*, 185–217. https://doi.org/10.1002/2013RG000431

Mogensen, K., Balmaseda, M. A., & Weaver, A. (2012). The NEMOVAR ocean data assimilation system as implemented in the ECMWF ocean analysis for System 4. ECMWF Technical Memorandum. 02/2012: 668.

Mori, M., Kosaka, Y., Watanabe, M., Nakamura, H., & Kimoto, M. (2019). A reconciled estimate of the influence of Arctic sea-ice loss on recent Eurasian cooling. *Nature Climate Change*, *9*, 123–129. https://doi.org/10.1038/s41558-018-0379-3

Mori, M., Watanabe, M., Shiogama, H., Inoue, J., & Kimoto, M. (2014). Robust Arctic sea-ice influence on the frequent Eurasian cold winters in past decades. *Nature Geoscience*, *7*, 869–873. https://doi.org/10.1038/ngeo2277

Overland, J. E., Dethloff, K., Francis, J. A., Hall, R. J., Hanna, E., Kim, S. J., et al. (2016). Nonlinear response of mid-latitude weather to the changing Arctic. *Nature Climate Change*, *6*, 992–999. https://doi.org/10.1038/nclimate3121

Overland, J. E., Hanna, E., Hanssen-Bauer, I., Kim, S.-J., Walsh, S.-J., Wang, M., et al. (2015). Surface air temperature, Arctic Report Card 2015.

Perovich, D., Meier, W., Tschudi, M., Farrell, S., Hendricks, S., Gerland, S., et al. (2019). Sea ice cover. Arctic report card, 2019 Update.

Pithan, F., & Mauritsen, T. (2014). Arctic amplification dominated by temperature feedbacks in contemporary climate models. *Nature Geoscience*, *7*, 181-184. https://doi.org/10.1038/ngeo2071

Post, E., Bhatt, U. S., Bitz, C. M., Brodie, J. F., Fulton, T. L., Hebblewhite, M., et al. (2013). Ecological consequences of sea-ice decline. *Science*, *341*, 519–524. https://doi.org/10.1126/science.1235225

Scaife, A. A., Arribas, A., Blockley, E., Brookshaw, A., Clark, R. T., Dunstone, N., et al. (2014). Skillful long range prediction of European and North American winters. *Geophysical Research Letters*, *41*, 2514–2519. https://doi.org/10.1002/2014GL059637

Screen, J. A., Deser, C., Smith, D. M., Zhang, X., Blackport, R., Kushner, P. J., et al. (2018). Consistency and discrepancy in the atmospheric response to Arctic sea-ice loss across climate models. *Nature Geoscience*, *11*, 155–163. https://doi.org/10.1038/s41561-018-0059-y

Semmler, T., Jung, T., Kasper, M. A., & Serrar, S. (2018). Using NWP to assess the influence of the Arctic atmosphere on midlatitude weather and climate. *Advances in Atmospheric Sciences*, *35*, 5–13. https://doi.org/10.1007/s00376-017-6290-4

Smith, D. M., Screen, J. A., Deser, C., Cohen, J., Fyfe, J. C., García-Serrano, J., et al. (2019). The Polar Amplification Model Intercomparison Project (PAMIP) contribution to CMIP6: Investigating the causes and consequences of polar amplification. *Geoscientific Model Development*, *12*, 1139–1164. https://doi.org/10.5194/gmd-12-1139-2019

Voldoire, A., Saint-Martin, D., Sénési, S., Decharme, B., Alias, A., Chevallier, M., et al. (2019). Evaluation of CMIP6 DECK experiments with CNRM-CM6-1. *Journal of Advances in Modeling Earth Systems*, *11*, 2177–2213. https://doi.org/10.1029/2019MS001683

Zhang, P., Wu, Y., & Smith, K. L. (2018). Prolonged effect of the stratospheric pathway in linking Barents–Kara Sea sea ice variability to the midlatitude circulation in a simplified model. *Climate Dynamics*, *50*, 527–539.

Zuo, H., Alonso Balmaseda, M., Tietsche, S., Mogensen, K., & Mayer, M. (2019). The ECMWF operational ensemble reanalysis-analysis system for ocean and sea-ice: A description of the system and assessment. *Ocean Science*, *15*, 779–808. https://doi.org/10.5194/os-15-779-2019